

Design, synthesis and photophysical studies of phenylethynyl-bridged phthalocyanine-fullerene dyads

Jaro Arero, Gerdenis Kodis, Robert A. Schmitz, Dalvin D. Méndez-Hernández, Thomas A. Moore*, Ana L. Moore* and Devens Gust*[‡]

Department of Chemistry and Biochemistry, Arizona State University, Tempe, AZ 85287, USA

Received 24 February 2015

Accepted 17 April 2015

ABSTRACT: A zinc and a free base phthalocyanine-fulleropyrrolidine dyad in which the chromophores are linked by a phenylethynyl group have been prepared using a new synthetic route, and their photoelectrochemical properties have been investigated. The zinc dyad is readily soluble in a variety of solvents, and its spectroscopic properties have been determined in toluene and benzonitrile. In toluene, excitation of the zinc phthalocyanine is followed by rapid establishment of an equilibrium between the phthalocyanine and fullerene excited states. These excited states decay mainly to the ground state and the respective triplet states. The fullerene triplet then transfers its energy to form the phthalocyanine triplet. About 20% of the phthalocyanine excited states lead to formation of a charge-separated state. In benzonitrile, the same decay pathways are observed, but photoinduced electron transfer is much faster, and generates the charge separated state with a quantum yield of $\geq 85\%$. The charge separated state has a lifetime of 2.8 ns in toluene and 94 ps in benzonitrile.

KEYWORDS: phthalocyanine, fullerene, dyad, synthesis, electron transfer.

INTRODUCTION

The initial chemical event in photosynthetic solar energy conversion is photoinduced electron transfer from an excited state donor to an acceptor. Since the late 1970's artificial photosynthetic reaction centers consisting of donor chromophores covalently linked to acceptors have been investigated as models for the natural process, and for possible applications in solar energy conversion [1–10]. Many of these donor–acceptor dyads, triads, *etc.* have featured porphyrins as the light absorbing electron donor. This is due to the resemblance of porphyrins to natural chlorophylls, their reasonably good light absorption, excited state lifetimes and redox properties, their high stability and lack of aggregation in solution, and the ease with which they can be synthesized

and their structures modified to tune properties. However, porphyrins do have drawbacks, and one of these is the relatively weak absorption by the Q-bands in the red spectral region. Because of relatively low extinction coefficients in this region, where there is abundant sunlight, porphyrins alone are not ideal light harvesters for efficient artificial photosynthesis.

Phthalocyanines (Pc), on the other hand, have very strong absorption in the Q-band region, typically 670–690 nm. Thus, they have the potential to absorb sunlight efficiently at those wavelengths, as do chlorophylls. In addition, although the presence of substituents at the β -positions of phthalocyanines generally has little effect on the Q-band absorption maxima, the position of these bands may be tuned by α -substitution [11]. The strong, long-wavelength Q-band absorption makes phthalocyanines attractive candidates for artificial photosynthesis. However, less research has been done in the area, relative to porphyrins, due to difficulties in synthesis and the tendency of phthalocyanines to aggregate and be insoluble.

In recent years, several research groups have begun investigating the use of phthalocyanines in artificial

[‡]SPP full member in good standing

*Correspondence to: Devens Gust, email: gust@asu.edu, tel: +1 480-965-4547; Thomas A. Moore, email: tmoore@asu.edu, tel: +1 480-965-3308; Ana L. Moore, email: amoore@asu.edu, tel: +1 480-965-2953

photosynthesis [12–40]. Since our initial synthesis and study of a porphyrin–fullerene dyad as an artificial reaction center [41], fullerenes (*e.g.* C₆₀) have been very popular as electron acceptor components in donor–acceptor assemblies, and the vast majority of the work with phthalocyanines has employed this acceptor. In general, phthalocyanine–fullerene dyads display photoinduced electron transfer to generate a Pc^{•+}–C₆₀^{•-} charge separated state. In most Pc–C₆₀ dyads the lifetime of this state is rather short (on the time scale of some ps). This is due in part to the relatively short chemical linkers which have been employed between the moieties, which favor rapid recombination. Long lifetimes for such states are desirable if one wishes to harvest the redox potential stored within them to make electricity or useful compounds such as fuels. Recently, Quintiliani and coworkers [14] reported a dyad consisting of a zinc phthalocyanine linked through a β-position to a fulleropyrrolidine *via* an ethynyl group. Upon excitation in benzonitrile, this molecule generated a charge-separated state with a lifetime of 36 ps and a quantum yield of 0.36. Longer lifetimes were observed in other solvents.

Electron transfer theory predicts that decreasing the electronic coupling between donor and acceptor (for example, by increasing the length of a linker between them) will reduce the rate constant for electron transfer. With the goal of increasing the lifetime of a Pc^{•+}–C₆₀^{•-} charge-separated state while maintaining a respectable quantum yield for its formation, we have synthesized Pc–C₆₀ dyad **1** and its zinc analog **1Zn** (Fig. 1), wherein the phthalocyanine and fulleropyrrolidine are linked by a phenylacetylene, and studied the photochemical properties of these molecules.

RESULTS AND DISCUSSION

Synthesis

The synthesis of dyad **1Zn** by a significantly different method was previously reported by Bottari *et al.* [42]. The synthesis of the dyads employed here is diagrammed in Fig. 1. Phthalonitrile **2** was synthesized by a literature method [18] involving Sonogashira coupling of 4-iodophthalonitrile with 4-ethynylbenzyl alcohol in the presence of [Pd(PPh₃)₂Cl] and CuI as the catalyst. Unsymmetrical ZnPc **3** was obtained by a statistical condensation reaction between **2** and 4-*t*-butylphthalonitrile in *N,N*-dimethylaminoethanol, which were heated at reflux in the presence of Zn(OAc)₂•2H₂O. Thin-layer chromatography (TLC) of the crude product showed two main products: the less polar zinc(II) tetra-*t*-butylphthalocyanine side product and the desired ZnPc **3**. Due to the significant polarity difference between the two products, separation was easily achieved by using silica column chromatography to yield **3** (17%). As is the case with all phthalocyanines of this general type, the product

is actually an inseparable mixture of isomers with the *t*-butyl groups distributed among the 6 β-positions. The hydroxyl functionality on **3** was oxidized to a formyl group by 2-iodoxybenzoic acid dissolved in a dimethyl sulfoxide/tetrahydrofuran mixture at room temperature to yield ZnPc **4** (79%). Synthesis of ZnPc–C₆₀ dyad **1Zn** from **4** was achieved by a 1,3-dipolar cycloaddition of azomethine yield generated *in situ* in a Prato reaction. Reaction between **4**, C₆₀ and sarcosine in refluxing toluene afforded a 53% yield of dyad **1Zn** after silica gel column purification.

For the synthesis of **1**, **4** was heated in a mixture of pyridine and pyridine hydrochloride at 120 °C for 24 h to yield Pc **5** essentially quantitatively (98%) without the need for column purification. Then, a 1,3-dipolar cycloaddition between **5**, C₆₀ and sarcosine was carried out to obtain Pc–C₆₀ dyad **1** in 69% yield, after silica gel column purification. Note that **1** and **1Zn** are racemic mixtures due to the presence of the stereocenter on the pyrrolidine moiety.

Model free base phthalocyanine **6** (Fig. 2) was prepared by removal of the zinc from **3**. A portion of **3** was heated in pyridine and pyridine–HCl at 120 °C for 21 h, followed by addition of water to the reaction mixture, cooling, centrifugation and filtration (38% yield).

Fulleropyrrolidine **7** (Fig. 2) was prepared by the Prato reaction of 4-anisaldehyde, sarcosine and C₆₀. Compound **7** was then demethylated by treatment with boron tribromide in a mixture of dichloromethane and toluene to give model fullerene **8**. Details of all syntheses and characterization of the products are given in the Experimental section.

Electrochemistry

The redox potentials of the dyads and model compounds were measured by cyclic voltammetry in order to allow estimation of the energies of charge separated states and driving force values for electron transfer reactions. Cyclic voltammetry was carried out in benzonitrile solution containing 0.10 M tetra-*n*-butylammonium hexafluorophosphate as supporting electrolyte. The experiments were performed in a one-compartment cell with a three-electrode configuration consisting of a glassy carbon working electrode, a Pt counter electrode, and an Ag⁺/Ag quasireference electrode. Voltammograms were measured in benzonitrile containing 100 mM tetrabutylammonium hexafluorophosphate after deoxygenation with argon, and using a scan rate of 20 mV/s. Potentials were converted to SCE by using ferrocenium/ferrocene (0.45 V *vs.* SCE) as an internal reference.

The results of the cyclic voltammetry are shown in Table 1. Useful results could not be obtained for dyad **1** due to aggregation and lack of solubility in benzonitrile. Table 1 indicates that the first oxidation potential for **1Zn** is 0.54 V *vs.* SCE, whereas that for model Pc **6** is

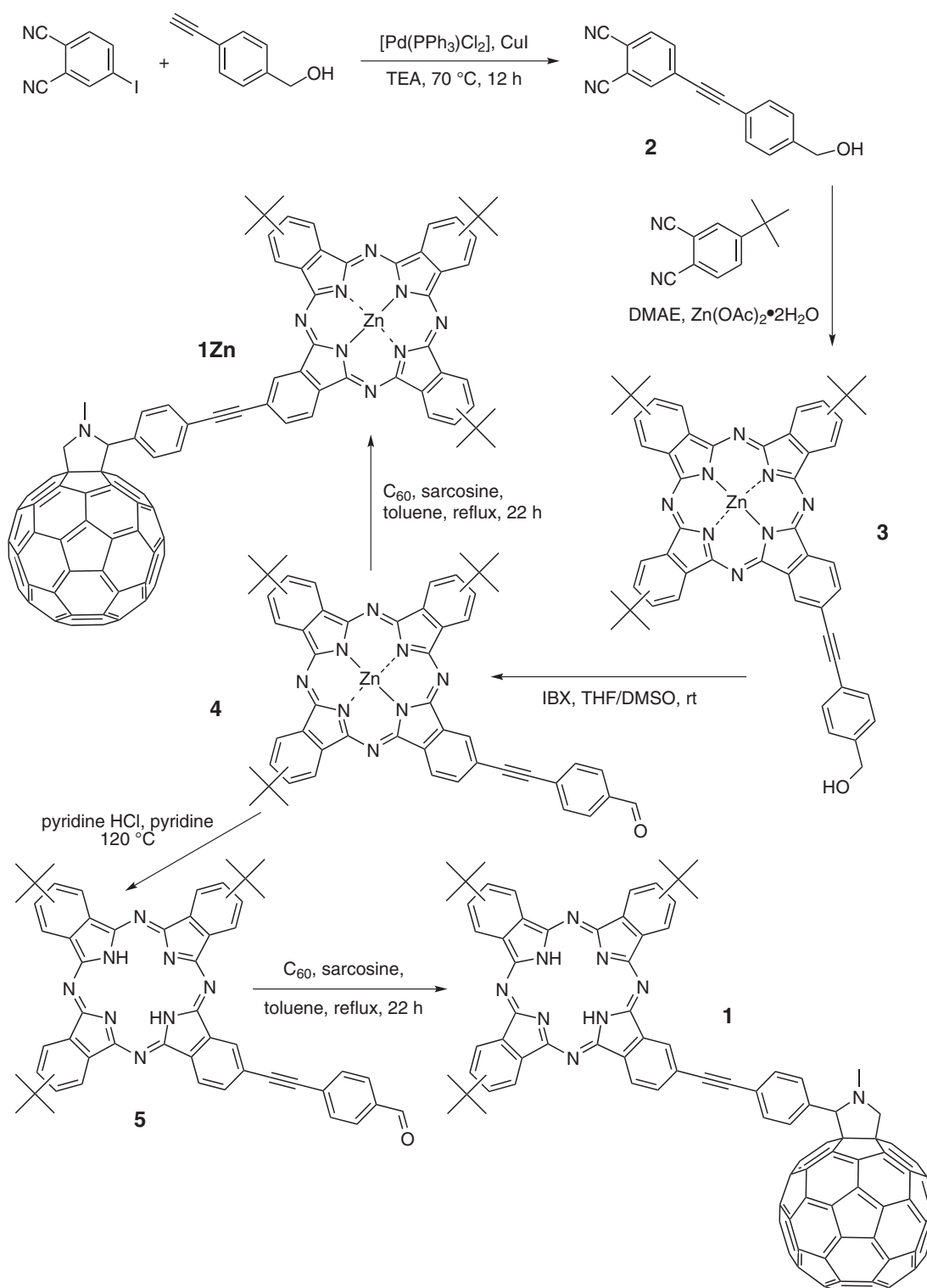


Fig. 1. Synthesis of dyads **1** and **1Zn**. TEA = triethylamine, DMAE = *N,N*-dimethylaminoethanol, IBX = 2-iodoxybenzoic acid, DMSO = dimethylsulfoxide, THF = tetrahydrofuran

0.59 V. Thus, this oxidation is ascribed to formation of the phthalocyanine radical cation. Similarly, the first reduction potential of **1Zn** is -0.66 V, whereas that of model C_{60} **8** is -0.63 V. Thus the -0.66 V feature in the CV of **1Zn** is due to formation of the fullerene radical

anion. These results show that linking the two moieties has little effect on their redox potentials. These data also permit estimation of the energy of the $\text{ZnPc}^{+\bullet}-\text{C}_{60}^{\bullet-}$ charge separated state of **1Zn** in benzonitrile as 1.20 eV above the ground state. The very small perturbations of the

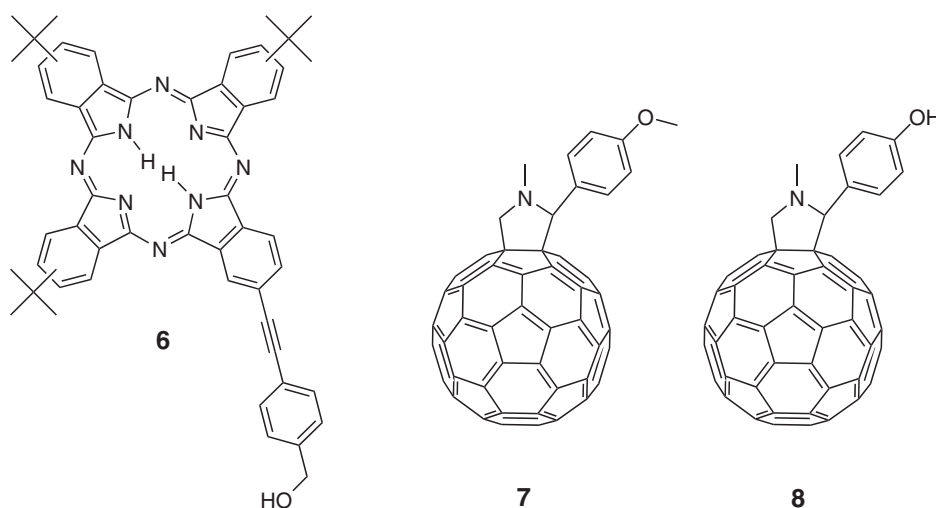


Fig. 2. Structures of model zinc phthalocyanine **6**, pyrrolidinofullerene intermediate **7** and model pyrrolidinofullerene **8**

Table 1. Cyclic voltammetric data in benzonitrile

Compound	1st oxidation in V vs. SCE and (peak width in mV)	1st reduction in V vs. SCE and (peak width in mV)
Pc model 6	0.62 (160)	-0.78 (54)
C ₆₀ model 8	—	-0.63 (80)
ZnPc model 3	0.59 (145)	-0.99 (90)
ZnPc-C ₆₀ 1Zn	0.54 (210)	-0.66 (74)

redox potentials observed upon linking the donor and acceptor moieties to form **1Zn** suggest that although the potentials for **1** could not be measured directly, they will be similar to those measured for model Pc **6** and model fullerene **8**. Thus, the energy of Pc^{•+}-C₆₀^{•-} in **1** is estimated to be *ca.* 1.25 eV above the ground state.

Spectroscopy

Steady-state spectroscopy. Due to the tendency of **1** to aggregate in solution, spectroscopic studies were carried out only on the zinc dyad and related model compounds. Figure 3 shows the absorption spectra of ZnPc **3**, model fullerene **8**, and ZnPc-C₆₀ dyad **1Zn** in benzonitrile. The two ZnPc spectra have been normalized at the Q-band maxima. The fullerene absorption spectrum is shown at a similar concentration. Model ZnPc **3** has a B-band absorption at 356 nm and Q-band maxima at 617, 641, 680 and 692 nm. In **1Zn**, the B-band appears at 352 nm and Q-band maxima at 617, 639, 680 and 694 nm. Model fullerene **8** shows broad absorption throughout the visible region, with strong absorption in the UV around 320 nm and a long wavelength maximum at 706 nm. The spectrum of the dyad is similar to a linear combination of the spectra of the two components with small differences in the 320 nm region that indicate weak interactions between the chromophores. Although the fullerene

moiety has absorbance out to 706 nm, it contributes significantly to the spectrum only in the UV region. The spectrum of **1Zn** in toluene solution (not shown) is very similar to that in benzonitrile, but with a small shift to shorter wavelengths; it has phthalocyanine maxima at 346, 613, 634, 675 and 689 nm and a small fullerene maximum at 702 nm.

Figure 4a shows the fluorescence emission spectra of the molecules in benzonitrile. The amplitudes at the maxima have been normalized. Model zinc phthalocyanine **3** shows an emission maximum at 711 nm with a weak shoulder around 735 nm and another maximum at 776 nm. Fullerene **8** has a somewhat similar emission, but with the long-wavelength maximum further into the infrared (maxima at 719 nm and ~756 nm). Dyad **1Zn** emission shows a maximum at 713 nm, a weak shoulder around 735 nm and another maximum at 774 nm. Figure 4b shows the emission spectra of **1Zn** in both benzonitrile and toluene; the absorbance of the two solutions was identical at the excitation wavelength. The spectral shapes are similar in both solvents, but the emission in benzonitrile is quenched by a factor of *ca.* 13. This indicates that in benzonitrile, a nonradiative pathway for decay of the excited state(s) has become more important.

The emission spectrum of **1Zn** resembles that of **3**, but is relatively more intense at wavelengths between

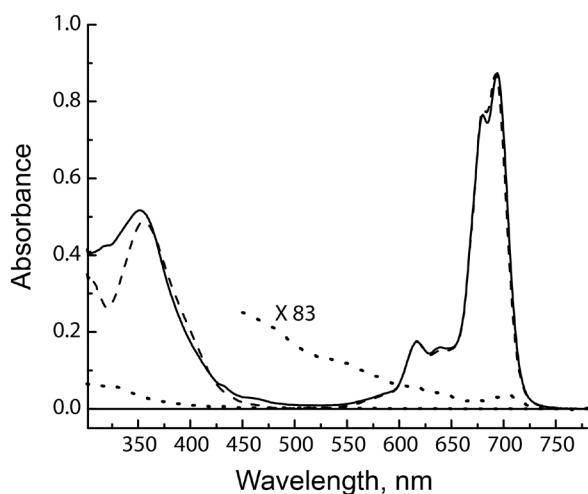


Fig. 3. Absorption spectra in benzonitrile of dyad **1Zn** (solid), model zinc phthalocyanine **3** (dashes) and model fullerene **8** (dots). A portion of the fullerene spectrum is also shown expanded by a factor of 83 along the absorbance axis

ca. 725 nm and 830 nm (Fig. 4a). The fullerene emits in this spectral region, but has very little absorption at the excitation wavelength, relative to that of the phthalocyanine. These facts suggest that the emission spectrum of the dyad features fluorescence from both the fullerene and the phthalocyanine, and the fullerene excited singlet state is populated mainly by singlet-singlet energy transfer from the phthalocyanine. This is reasonable, because the two excited states are nearly isoenergetic, and the chromophores are separated by a short distance that should permit energy transfer by the Förster mechanism [43].

Transient absorption spectroscopy. In order to learn more about the excited state behavior of **1Zn**, ps transient absorption measurements were performed on **1Zn** in a toluene solution that was deoxygenated by bubbling with argon. Excitation was at 695 nm, near the ZnPc maximum, with ca. 100 fs laser pulses. At this wavelength, essentially all of the excitation leads to initial formation of $^1\text{ZnPc-C}_{60}$. The results obtained are shown in Fig. 5a as decay-associated spectra, where each spectrum is associated with a particular decay time. Four decay components were observed. The shortest, with a time constant of 1.1 ps, has a negative amplitude in the 690 nm region and positive amplitude around 700 nm, and is ascribed to a bathochromic shift of the ZnPc stimulated emission due to excited singlet state relaxation and solvation. The decay lifetimes of 52 ps and 1.24 ns both show similar ground state bleaching and stimulated emission in the 660–780 nm range. These decays reflect both the ZnPc and fullerene excited singlet states. These transients are associated with the singlet-singlet energy transfer between the phthalocyanine and the fullerene discussed above; following excitation of the ZnPc moiety, a pseudoequilibrium is established by the

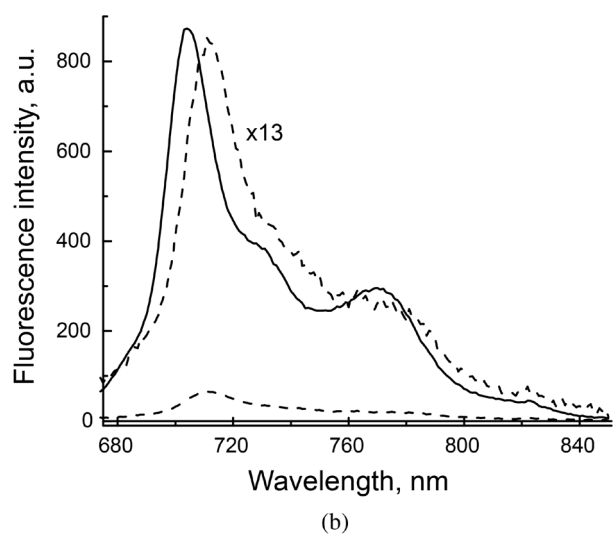
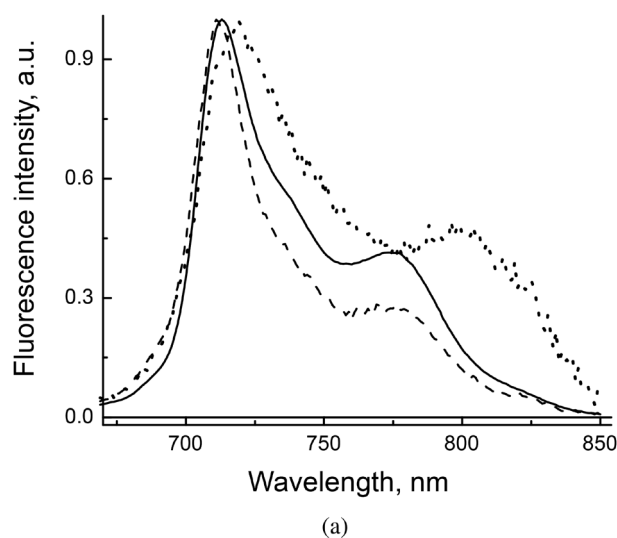


Fig. 4. Corrected fluorescence emission spectra for (a) model phthalocyanine **3** (dash) with excitation at 300 nm, and model fullerene **8** (dot) and dyad **1Zn** (solid) with excitation at 430 nm in benzonitrile, with all spectra normalized at the maxima, and (b) dyad **1Zn** in toluene (solid) and in benzonitrile (dash), obtained with equal absorption at the excitation wavelength (547 nm). The spectrum in benzonitrile is also shown multiplied by 13 along the emission axis

two excited states, which then both decay concurrently to yield the $\text{ZnPc}^{*+}\text{-C}_{60}^{*-}$ charge separated state (giving rise to the ZnPc^{*+} induced absorption at ~550 and ~860 nm) and the ground and triplet states of both moieties. The energy of $^1\text{ZnPc}$ in toluene is estimated to be 1.78 eV above the ground state from the wavenumber average of the longest-wavelength absorption maximum and the shortest-wavelength emission maximum. Similarly, the fullerene first excited singlet state lies at 1.75 eV. These values give an equilibrium constant of 3.1 for singlet-singlet energy transfer between the phthalocyanine and fullerene excited singlet states.

The longest decay time is longer than could be determined using the conventional fs-ns apparatus

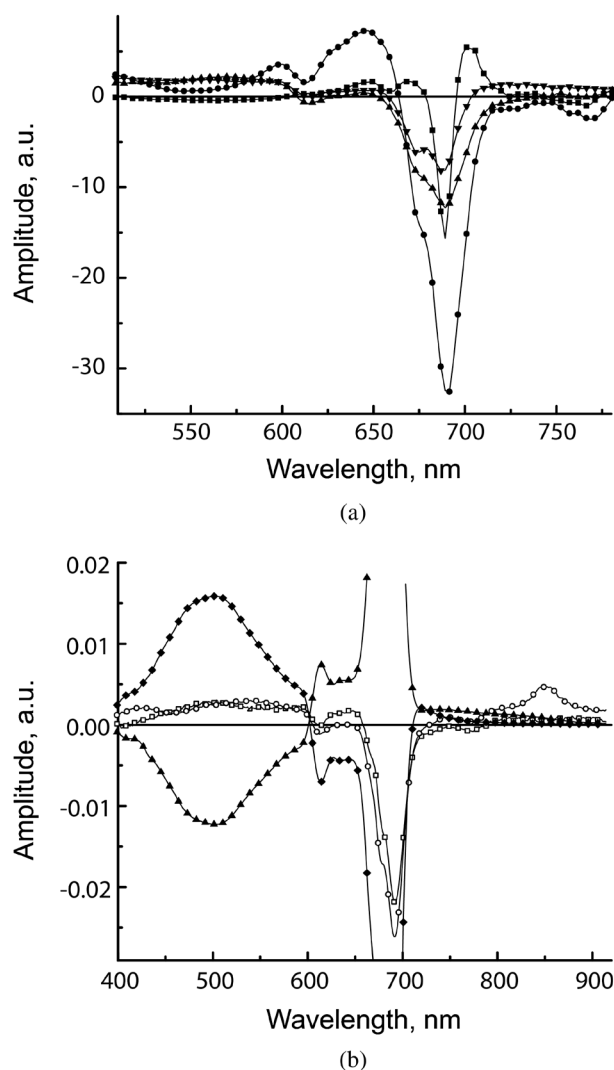


Fig. 5. (a) Transient absorption decay associated spectra of dyad **1Zn** in toluene on the fs-ns time scale, with excitation at 695 nm. The time constants associated with the decays are 1.1 ps (squares), 52 ps (circles), 1.24 ns (triangles) and a value too long to determine on the time scale of this measurement (inverted triangles). (b) Transient absorption decay associated spectra of dyad **1Zn** in toluene on the ns- μ s time scale. The time constants associated with these decays are 1.24 ns (hollow squares), 2.81 ns (hollow circles), 46.6 ns (triangles) and 2.5 μ s (diamonds)

(IRF \sim 150 fs, optical delay line \leq 3 ns). We therefore investigated the material on the ns-ms time scale using an EOS spectrometer from Ultrafast Systems (IRF \sim 800 ps). Excitation at 670 nm of an argon-bubbled toluene solution of **1Zn** with *ca.* 100 fs pulses gave the decay associated spectra shown in Fig. 5b. The 1.24 ns decay associated spectrum is the same decay that was observed on the ps time scale. The 2.81 ns decay shows ground state bleaching at \sim 690 nm and induced absorption at \sim 550 nm and \sim 860 nm that are characteristic of the ZnPc radical cation, and therefore can be associated with the decay of the $\text{ZnPc}^{\bullet+}\text{-C}_{60}^{\bullet-}$ charge-separated state. The 46.6 ns decay associated spectrum shows decay of

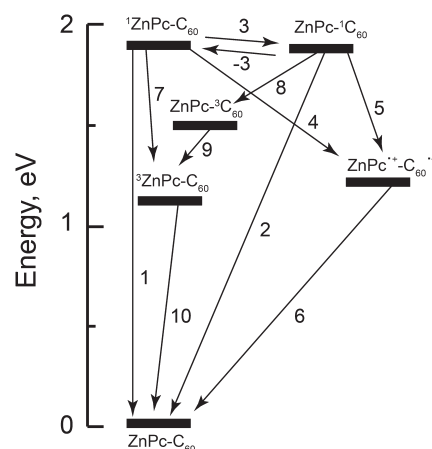


Fig. 6. Energy diagram showing ground and transient high energy states of dyad **1Zn** and their interconversion pathways. Values for the rate constants for the various steps indicated are given in the text for two solvents

induced absorption at \sim 700 nm, which is due to decay of the C_{60} triplet state, and the formation of ground state bleaching at \sim 690 nm and induced absorption at \sim 500 nm are due to formation of the ZnPc triplet state. Thus, this component represents triplet-triplet energy transfer from the fullerene triplet to the zinc phthalocyanine. Finally, the 2.5 μ s spectrum represents decay of $^3\text{ZnPc}$.

The excited state behavior of **1Zn** in toluene can be discussed with reference to Fig. 6, which shows the various states of interest and pathways for interconversion between them. The energies of the fullerene triplet state (\sim 1.50 eV) [44] and the zinc phthalocyanine triplet state (1.13 eV) [45] are based on literature values for similar molecules. When two excited states are in equilibrium with energy transfer rate constants k_3 and k_{-3} (for steps 3 and -3 in Fig. 6) and each decays by the usual photophysical pathways to the ground state with rate constants k_1 and k_2 and the triplet state with k_7 and k_8 , transient behavior will feature two time constants τ_A and τ_B with associated rate parameters γ_A and γ_B [46]. As indicated in Equations 1 and 2, these rate parameters may be related to the rate constants in Fig. 6, where the values of X and Y are as given in Equations 3 and 4.

$$Y_A = \{(X+Y) + [(X-Y)^2 + 4k_3k_{-3}]^{1/2}\} / 2 \quad (1)$$

$$Y_B = \{(X+Y) - [(X-Y)^2 + 4k_3k_{-3}]^{1/2}\} / 2 \quad (2)$$

$$X = k_1 + k_7 + k_4 + k_{3+} \quad (3)$$

$$Y = k_2 + k_8 + k_5 + k_{-3} \quad (4)$$

The values of γ_A and γ_B are the reciprocals of the 52 ps and 1.24 ns decays observed in the decay-associated spectra. The sum of k_1 and k_7 may be taken as the reciprocal of the excited singlet state lifetime of model ZnPc **3**. This lifetime was measured in toluene by time correlated

single photon counting fluorescence measurements, and equals 2.91 ns. Similarly, the lifetime of $^1\text{C}_{60}$ in model **8** was found to be 1.34 ns, and its reciprocal equals $k_2 + k_8$. The equilibrium constant for singlet energy transfer, K , is 3.1, as mentioned above, and thus $k_{-3} = k_3/3.1$. We are therefore left with two equations and three unknowns, k_3 , k_4 and k_5 . Electron transfer steps 4 and 5 involve the same two chromophores and the same linkage between them. The driving force for electron transfer is very nearly the same for the two reactions, given the small difference in energies of the initial states, and the fact that the final state is the same in both cases. However, the orbitals involved are different, as step 4 involves transfer of an electron between LUMOs, and step 5 is “hole transfer” involving HOMOs. In the absence of other information, we will assume that the electronic coupling is approximately the same for the two reactions, and that $k_4 = k_5$. Making this assumption allows us to solve Equations 1–4 [47] to yield values of $k_3 = 1.4 \times 10^{10} \text{ s}^{-1}$ ($\tau_3 = 71 \text{ ps}$), $k_{-3} = 4.6 \times 10^9 \text{ s}^{-1}$ ($\tau_{-3} = 220 \text{ ps}$), and $k_4 = k_5 = 1.6 \times 10^8 \text{ s}^{-1}$ ($\tau_4 = \tau_5 = 6.3 \text{ ns}$). Based on these values, the total quantum yield of charge separation in toluene is *ca.* 20%. From the time-resolved data above, we find that k_6 , rate constant for charge recombination of $\text{ZnPc}^{*+}\text{-C}_{60}^{*\bullet}$ is $3.6 \times 10^8 \text{ s}^{-1}$ (the reciprocal of 2.81 ns). Thus, charge recombination is slightly faster than charge separation. The rate constant for transfer of triplet energy from the fullerene to the phthalocyanine, k_9 , is $2.2 \times 10^7 \text{ s}^{-1}$ ($\tau = 46.6 \text{ ns}$), and k_{10} , the rate of decay of the phthalocyanine triplet to the ground state, is $4.0 \times 10^5 \text{ s}^{-1}$ ($\tau = 2.5 \mu\text{s}$). It is likely that this lifetime is shortened due to small amounts of residual oxygen in the sample. In summary, in toluene $^1\text{ZnPc-C}_{60}$ is in equilibrium with $\text{ZnPc-}^1\text{C}_{60}$ by singlet–singlet energy transfer, and both excited states decay to yield the $\text{ZnPc}^{*+}\text{-C}_{60}^{*\bullet}$ charge-separated state, their corresponding triplet states, and their ground states. $\text{ZnPc-}^3\text{C}_{60}$ decays by triplet energy transfer to yield $^3\text{ZnPc-C}_{60}$, which lies at significantly lower energy.

The steady-state fluorescence results above show that in benzonitrile, the excited state lifetimes of both the zinc phthalocyanine and fullerene chromophores of **1Zn** are significantly shorter than they are in toluene. In order to investigate the reasons for this behavior, we obtained the transient absorption decay associated spectra for **1Zn** in benzonitrile with excitation at 695 nm, and the results are plotted in Fig. 7. Three time constants were observed: 1.3 ps, 10 ps and 94 ps. The 10 ps component shows decay of phthalocyanine stimulated emission in the 690–780 nm spectral region and decay of phthalocyanine excited singlet state induced absorption in the 600–680 nm region, all of which are consistent with decay of $^1\text{ZnPc}$. This decay associated spectrum also features negative amplitude around 560 nm, which is due to the formation of induced absorption due to ZnPc^{*+} . Thus, the 10 ps component is associated mainly with formation of the $\text{ZnPc}^{*+}\text{-C}_{60}^{*\bullet}$ charge-separated state by photoinduced electron transfer from $^1\text{ZnPc-C}_{60}$. The 94 ps decay

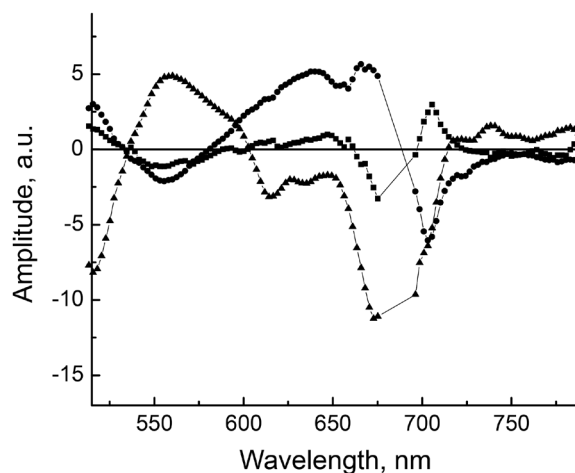


Fig. 7. Decay associated spectra from excitation of **1Zn** in benzonitrile at 695 nm. The time constants are 1.3 ps (squares), 10 ps (circles) and 94 ps (triangles)

associated spectrum shows ground state bleaching at ~600–700 nm and <540 nm due to the ZnPc^{*+} and $\text{C}_{60}^{*\bullet}$ radical ions. There is also induced absorption at ~560 nm that is characteristic of ZnPc^{*+} , and no stimulated emission is observed. Thus, this decay is associated with the decay of the $\text{ZnPc}^{*+}\text{-C}_{60}^{*\bullet}$ charge-separated state to the ground state. The 1.3 ps component has negative amplitude at ~690 nm and positive amplitude at ~700 nm due to the bathochromic shift of the ZnPc stimulated emission that results from excited state relaxation and solvation, as was observed in toluene. This component also shows some negative amplitude at ~560 nm, which may be ascribed to some very rapid formation of $\text{ZnPc}^{*+}\text{-C}_{60}^{*\bullet}$ from the unrelaxed ZnPc excited state.

We will discuss this behavior with reference to Fig. 6, as was done for the results in toluene. The energies of $^1\text{ZnPc-C}_{60}$ and $\text{ZnPc-}^1\text{C}_{60}$ are estimated to be 1.76 and 1.74 eV, respectively, in benzonitrile. Photoinduced electron transfer from $^1\text{ZnPc-C}_{60}$ to yield $\text{ZnPc}^{*+}\text{-C}_{60}^{*\bullet}$ (step 4) is much more rapid in benzonitrile than in toluene, and dominates the decay of $^1\text{ZnPc-C}_{60}$. The rate constant for step 4 may be estimated according to Equation 5, where $\tau_{1\text{Zn}}$ = the 10 ps lifetime of the first excited singlet state of $^1\text{ZnPc-C}_{60}$;

$$k_4 = \frac{1}{\tau_{1\text{Zn}}} - \frac{1}{\tau_1} - k_3 \quad (5)$$

τ_1 is taken as the excited state lifetime of $^1\text{ZnPc}$ in model compound **3**, which has been found to be 2.64 ns in benzonitrile *via* fluorescence decay measurements, and k_3 is the rate constant for singlet–singlet energy transfer from $^1\text{ZnPc-C}_{60}$ to yield $\text{ZnPc-}^1\text{C}_{60}$. Because rate constants for energy transfer show only a weak solvent dependence, we will take the value of k_3 as $1.4 \times 10^{10} \text{ s}^{-1}$, as calculated above for toluene. This yields a value for k_4 of $8.5 \times 10^{10} \text{ s}^{-1}$, and a quantum yield of photoinduced

electron transfer of 85% from this process. Equation 5 ignores any contribution from k_3 . The fate of the small amount of $\text{ZnPc}^+\text{-C}_{60}$ excited state that results from energy transfer is unknown, but it is likely that it decays mainly to $\text{ZnPc}^{*+}\text{-C}_{60}^{\bullet}$, for the reasons mentioned above. In any case, no time constant corresponding to the unperturbed lifetime of the fullerene excited state (1.40 ns in benzonitrile) was observed. The rate constant for charge recombination step 6 is $k_6 = 1.06 \times 10^{10} \text{ s}^{-1}$, as calculated from the 94 ps decay time.

Discussion

A new synthetic approach for the preparation of phenylethynyl-bridged zinc and free base phthalocyanine-fullerene dyads has been developed. Statistical condensation of functionalized phthalonitrile **2** with 4-*tert*-butylphthalonitrile yields zinc phthalocyanine **3**, which bears a 4-ethynylbenzyl alcohol group. This zinc phthalocyanine can be easily separated from the reaction mixture. The benzyl alcohol functionality is then converted to the corresponding aldehyde by use of a mild oxidant, 2-iodoxybenzoic acid, to afford **4**, which serves as a common intermediate for both the zinc and free base dyads. Dyad **1Zn** was prepared directly from **4** in a Prato-type reaction with sarcosine and C_{60} . Synthesis of free base dyad **1** was achieved *via* a quantitative demetallation of **4** using pyridine-HCl/pyridine to afford free base aldehyde **5**, which also underwent a 1,3-dipolar cycloaddition with C_{60} and sarcosine to form **1**. This is the first report of the preparation of **1**. Dyad **1Zn** was prepared previously by a different route in which aldehyde **4** was made from a tri-*tert*-butylidophthalocyanine using a Sonogashira coupling reaction with 4-ethynylbenzaldehyde [42].

The spectroscopic results show that in toluene, $^1\text{ZnPc-C}_{60}$ decays into an equilibrium with $\text{ZnPc}^+\text{-C}_{60}$, and that the resulting excited states decay mainly to the ground and triplet states, although about 20% of the excited states undergo photoinduced electron transfer to yield $\text{ZnPc}^{*+}\text{-C}_{60}^{\bullet}$. In benzonitrile, on the other hand, $^1\text{ZnPc-C}_{60}$ decays to give mainly $\text{ZnPc}^{*+}\text{-C}_{60}^{\bullet}$. About 14% of the decay is by energy transfer to yield $\text{ZnPc}^+\text{-C}_{60}$, which likely also decays to $\text{ZnPc}^{*+}\text{-C}_{60}^{\bullet}$. Overall the yield of the charge-separated state is $\geq 85\%$.

The rate constant for photoinduced electron transfer in benzonitrile is 53 times that in toluene, whereas the rate constant for charge recombination in benzonitrile is 30 times faster than that in toluene. The electron transfer rates can be discussed in terms of the Marcus-Hush theory of electron transfer [48–52]. For a given dyad molecule in different solvents, differences in rate constants are due mainly to differences in solvent reorganization energy and to differences in solvent stabilization of the charge-separated state, which affect the thermodynamic driving force for electron transfer. The driving force for photoinduced electron transfer in benzonitrile may be estimated from the energy of $^1\text{ZnPc-C}_{60}$ (1.76 eV)

and the energy of $\text{ZnPc}^{*+}\text{-C}_{60}^{\bullet}$ as estimated from cyclic voltammetry in the same solvent (1.20 eV) as 0.56 eV. The driving force for charge recombination to the ground state is 1.20 eV. Charge recombination in benzonitrile is slower than charge separation even though the driving force for recombination is greater because the photoinduced electron transfer reaction lies in the normal region of the Marcus rate constant *vs.* free energy change relationship, whereas charge recombination likely lies in the inverted region. In toluene, the driving force for photoinduced electron transfer is expected to decrease, due to loss of solvent stabilization of the very polar charge-separated state. This will decrease the rate of charge separation because the reaction lies in the normal region. But the solvent reorganization energy will decrease, which will act to increase the rate of charge separation. In **1Zn**, the reorganization effect is evidently outweighed by the contribution from the free-energy change. In charge recombination, changing the solvent from benzonitrile to toluene increases the driving force for charge recombination because the charge separated state is less stable, and this is expected to slow the rate of charge recombination in the inverted region. This is observed. The decrease in solvent reorganization energy in the less polar toluene is also expected to slow charge recombination in the inverted region, as observed.

In a recent very brief note concerning the photochemistry of **1Zn** by Guldi, Torres and coworkers [24], it was stated that excitation of **1Zn** in toluene yielded $^1\text{ZnPc-C}_{60}$, which decayed with a time constant of 30 ps to give the $\text{ZnPc}^{*+}\text{-C}_{60}^{\bullet}$ charge separated state, which decayed with a time constant of approximately 30 ns. Detailed spectra were not provided. As mentioned above, our study also reveals some photoinduced electron transfer in toluene, but indicates that the vast majority of $^1\text{ZnPc-C}_{60}$ decays to an equilibrium with $\text{ZnPc}^+\text{-C}_{60}$ by singlet-singlet energy transfer, and that the two excited states then decay mainly to the ground state and a long-lived triplet state in ~ 2.8 ns. The complex photochemical behavior of **1Zn** in toluene is not apparent unless a thorough study of the spectra at many wavelengths and time scales is available.

A report by Guldi, Torres, Hieringer and coworkers [14] has reported results for a zinc phthalocyanine-fullerene dyad with a structure similar to that of **1Zn**, but lacking the phenyl group between the fulleropyrrolidine and the triple bond. They report that in that molecule, excitation of the phthalocyanine moiety in benzonitrile leads rapidly to the formation of a $\text{ZnPc}^{*+}\text{-C}_{60}^{\bullet}$ charge-separated state. The time constant for photoinduced electron transfer is not given, but the quantum yield was reported as 0.56. The lifetime of $\text{ZnPc}^{*+}\text{-C}_{60}^{\bullet}$ was 36 ps. The shorter lifetime for the charge-separated state, as compared to the 94 ps found in **1Zn**, is consistent with the shorter chemical linkage joining the chromophores, which in turn would lead to stronger electronic coupling and faster electron transfer. The thermodynamic driving force parameters for the two molecules are expected to be almost identical.

As might be expected, reducing the electronic coupling between the phthalocyanine and fullerene in different dyad architectures leads to an increase in the lifetime of the charge-separated state [16, 33].

EXPERIMENTAL

General analytical

The UV-visible spectroscopy employed a Shimadzu UV-3101PC UV-visible spectrophotometer. Mass spectrometry was performed by the MALDI-TOF method using a Voyager DE STR from Applied Biosystems in reflector mode. ^1H NMR spectra were obtained using a Varian 400 MHz instrument with tetramethylsilane as internal reference. Proton assignments were aided by the use of COSY experiments. Electrochemistry was carried out using CH Instruments 650C or 760D electrochemical workstations and a standard 3-electrode cell setup. Parameters were as described above.

Fluorescence

Steady-state fluorescence spectra were measured using a Photon Technology International MP-1 spectrometer and corrected for detection system response as a function of wavelength. Excitation was provided by a 75 W xenon-arc lamp and a single-grating monochromator. Fluorescence was detected at 90° to the excitation beam *via* a single-grating monochromator and an R928 photomultiplier tube having S-20 spectral response and operating in the single photon counting mode.

Fluorescence decay measurements were performed on optically dilute (*ca.* 1×10^{-5} M) samples by the time-correlated single-photon-counting method. The excitation source was a mode-locked Ti:Sapphire laser (Spectra Physics, Millennia-pumped Tsunami) with a 130-fs pulse duration operating at 80 MHz. The laser output was sent through a frequency doubler and pulse selector (Spectra Physics Model 3980) to obtain 370–450 nm pulses at 4 MHz. Fluorescence emission was detected at the magic angle using a double grating monochromator (Jobin Yvon Gemini-180) and a microchannel plate photomultiplier tube (Hamamatsu R3809U-50). The instrument response function was 35–55 ps. The spectrometer was controlled by software based on the LabView programming language and data acquisition was done using a single photon counting card (Becker-Hickl, SPC-830).

Transient absorption

The conventional femtosecond transient absorption apparatus consisted of a kilohertz pulsed laser source (adjustable up to sub-Hertz frequencies for EOS applications, *vide infra*) and a pump-probe optical setup. Laser pulses of 100 fs at 800 nm were generated from an amplified, mode-locked titanium sapphire laser system

(Millennia/Tsunami/Spitfire, Spectra Physics). Part of the laser pulse was sent through an optical delay line and focused on to a 3 mm sapphire plate to generate a white light continuum for the probe beam. The remainder of the pulse energy was used to pump an optical parametric amplifier (Spectra Physics) to generate excitation pulses, which were selected using a mechanical chopper. The white light generated was then compressed by prism pairs (CVI) before passing through the sample. The polarization of pump beam was set to the magic angle (54.7°) relative to the probe beam and its intensity adjusted using a continuously variable neutral density filter. The white light probe was dispersed by a spectrograph (300 line grating) onto a charge-coupled device (CCD) camera (DU420, Andor Tech.). The final spectral resolution was about 2.3 nm for over a nearly 300 nm spectral region. The instrument response function (IRF) was *ca.* 150 fs. Transient absorption spectra and kinetics on the ps-ms time scale were obtained using EOS spectrometer from Ultrafast Systems (IRF \sim 800 ps); excitation was from the same optical parametric amplifier as described above.

Data analysis was carried out using locally written software (ASUFIT) developed under a MATLAB environment (Mathworks Inc.). Decay-associated spectra (DAS) were obtained by fitting the transient absorption or fluorescence change curves over a selected wavelength region simultaneously as described by Equation 6 (parallel kinetic model),

$$\Delta A(\lambda, t) = \sum_{i=1}^n A_i(\lambda) \exp(-t/\tau_i) \quad (6)$$

where $\Delta A(\lambda, t)$ is the observed absorption (or fluorescence) change at a given wavelength at time delay t and n is the number of kinetic components used in the fitting. A plot of $A_i(\lambda)$ vs. wavelength is called a decay-associated spectrum, and represents the amplitude spectrum of the i th kinetic component, which has a lifetime of τ_i . The global analysis procedures described here have been extensively reviewed in literature [53]. Random errors associated with the reported lifetimes obtained from fluorescence and transient absorption measurements were typically $\leq 5\%$.

Synthesis

4-(2-(4-(Hydroxymethyl)phenyl)ethynylphthalonitrile (2). A 30-mL portion of Et_3N was placed in a round-bottomed flask immersed in ice-water and deoxygenated with argon for 40 min. A mixture of 4-ethynylbenzyl alcohol (126 mg, 0.953 mmol) and 4-iodophthalonitrile (219 mg, 0.862 mmol) was dissolved in the Et_3N . Next, $\text{Pd}(\text{PPh}_3)_2\text{Cl}_2$ (63 mg, 0.0898 mmol) and CuI (21 mg, 0.11 mmol) were added. The reaction mixture was stirred for 15 h at 70°C under the argon atmosphere. The solvent was then removed by distillation under reduced pressure and the crude product was purified by flash column chromatography on

silica gel (CH₂Cl₂/EtOAc, 9/1) to yield 207 mg (93%) of **2** as a white solid. ¹H NMR (CDCl₃, 400 MHz): δ, ppm 7.83 (s, 1 H), 7.75–7.69 (m, 2 H), 7.48–7.46 (d, *J* = 8 Hz, 2 H), 7.35–7.33 (d, *J* = 8 Hz, 2 H), 4.68 (s, 2 H), 1.85 (br s, 1 H).

Zinc phthalocyanine 3. A mixture of 4-*tert*-butylphthalonitrile (715 mg, 3.88 mmol), phthalonitrile **2** (200 mg, 0.775 mmol) and Zn(OAc)₂·2H₂O (825 mg, 3.76 mmol) in 30 mL of DMAE was stirred and heated at 130 °C for 24 h. The mixture was cooled to room temperature, the solvent was removed by distillation at reduced pressure, the residue was washed with MeOH/H₂O (5/1) and the dark green crude product obtained was purified by flash column chromatography on silica gel (toluene/THF, 9/1). The blue symmetrical phthalocyanine eluted first, followed by the greenish blue phthalocyanine **3** (119 mg, 17%). ¹H NMR (d₈-THF, 400 MHz): δ, ppm 10.02 (s, 1 H), 9.45–9.20 (m, 8 H), 8.33–8.27 (m, 3 H), 7.86–7.72 (m, 4 H), 4.71 (s, 2 H), 4.35 (br s, 1 H), 1.85–1.73 (m, 27 H). UV-vis (THF): λ_{max}, nm 683, 611 and 350. MALDI-TOF MS (terthiophene): *m/z* calcd. for C₅₃H₄₆N₈OZn [M]⁺ 874.38, found 874.75.

Zinc phthalocyanine 4. A mixture of phthalocyanine **3** (20 mg, 0.023 mmol) and iodoxybenzoic acid (20 mg, 0.0714 mmol) in THF (3 mL) and DMSO (3 mL) was stirred under an argon atmosphere at room temperature for 48 h. Stirring was stopped, 10 mL of brine was added to the mixture and the resulting solution was extracted with ether. The solvent was removed from the organic layer by distillation under reduced pressure and the crude product was purified by column chromatography toluene/THF (19/1) to yield green phthalocyanine **4** (16 mg, 79%). ¹H NMR (THF-*d*₈, 400 MHz): δ, ppm 9.99 (s, 1 H), 9.40–9.28 (m, 4 H), 9.22–9.11 (m, 4 H), 8.22–8.15 (m, 4 H), 7.96–7.86 (m, 4 H), 1.75–1.62 (m, 27 H). UV-vis (THF): λ_{max}, nm 687, 672, 611, 352. MALDI-TOF MS (terthiophene): *m/z* calcd for C₅₃H₄₄N₈OZn [M]⁺ 872.29, found 874.49.

Zinc phthalocyanine-C₆₀ dyad (1Zn). A mixture of phthalocyanine **4** (15 mg, 0.017 mmol), C₆₀ (41 mg, 0.057 mmol) and sarcosine (11 mg, 0.12 mmol) in anhydrous toluene (25 mL) was stirred at reflux for 22 h under an argon atmosphere. After this time the mixture was cooled and the solvent was removed by distillation under reduced pressure. The crude product was purified by column chromatography on silica gel (toluene/THF, 49/1) to obtain the phthalocyanine-C₆₀ dyad **1Zn** as a dark-blue powder (15 mg, 53%). ¹H NMR (THF-*d*₈, 400 MHz): δ, ppm 9.41–9.49 (m, 4 H), 9.31–9.23 (m, 4 H), 8.31–8.22 (m, 4 H), 7.98 (br s, 2 H), 7.87 (br s, 2 H), 5.06–5.01 (m, 3 H), 4.28–4.25 (d, *J* = 12 Hz, 2H), 2.86 (s, 3 H, N-CH₃), 1.94–1.76 (m, 27 H). UV-vis (THF): λ_{max}, nm 685, 672, 632, 610, 350. MALDI-TOF MS (dithranol): *m/z* calcd. for C₁₁₅H₄₉N₉Zn [M]⁺ 1620.34, found 1620.48.

Phthalocyanine 5. Phthalocyanine **4** (100 mg, 0.115 mmol), pyridine (10 mL) and pyridine-HCl (0.30 g)

were stirred under argon for 24 h. After this time stirring and heating were stopped and water (10 mL) was added to the hot mixture. The mixture was allowed to cool and the resulting precipitate was collected by centrifugation at 3,250 rpm. The bluish green precipitate was washed several times with water and then MeOH and dried under high vacuum to obtain phthalocyanine **5** (91 mg, 98%). ¹H NMR (THF-*d*₈, 400 MHz): δ, ppm 10.05 (s, 1 H), 8.70–7.19 (m, 16 H), 1.71–1.88 (m, 27 H). UV-vis (CH₂Cl₂): λ_{max}, nm 693, 677, 646, 620, 338. MALDI-TOF MS (terthiophene): *m/z* calcd. for C₅₃H₄₆N₈ [M]⁺ 810.38, found 810.55.

Phthalocyanine-C₆₀ dyad 1. A solution of phthalocyanine **5** (20 mg, 0.025 mmol), C₆₀ (59 mg, 0.082 mmol), and sarcosine (15.8 mg, 0.177 mmol) in anhydrous toluene (25 mL) was heated at reflux with stirring under an argon atmosphere for 22 h. After this time the solvent was removed by distillation under reduced pressure and the crude product was purified by column chromatography (toluene/CS₂, 1/1) to obtain **1** as a green solid (26.7 mg, 69%). ¹H NMR (toluene-*d*₈, 400 MHz): δ, ppm 9.14–8.65 (m, 9H), 7.96–7.68 (m, 7H), 4.77 (s, 1 H), 4.67–4.64 (d, *J* = 12 Hz, 1 H), 3.99–3.97 (d, *J* = 8 Hz, 1 H), 2.62 (s, 3 H, N-CH₃), 1.66–1.63 (m, 27 H), 2.29 (br s, 2 H). UV-vis (THF): λ_{max}, nm 694, 672, 644, 613, 343. MALDI-TOF MS (dithranol): *m/z* calcd. for C₁₁₅H₅₁N₉ [M]⁺ 1558.43, found 1558.80.

Phthalocyanine 6. Compound **3** (36 mg, 0.41 mmol), pyridine (10 mL) and pyridine-HCl (0.089 g) were heated at 120 °C while stirring under argon for 21 h. After brief cooling, water (5 mL) was added to the mixture. The mixture was allowed to cool, and the resulting precipitate was collected by centrifugation at 3,250 rpm. The green precipitate was washed several times with water and then MeOH and dried under high vacuum to obtain phthalocyanine **6** (12.7 mg 38%). ¹H NMR (toluene-*d*₈, 400 MHz): δ, ppm 8.94–8.37 (m, 10 H), 8.22–8.05 (m, 6 H), 4.67 (s, 2 H), 4.34 (br s, 1 H), 1.95–1.72 (m, 27 H). UV-vis (THF): λ_{max}, nm 694, 667, 644, 611, 344. MALDI-TOF MS (terthiophene): *m/z* calcd. for C₅₃H₄₈N₈O [M]⁺ 812.40, found 812.45.

N-methyl-2-(p-methoxyphenyl)-3, 4-fulleropyrrolidine 7. A mixture of C₆₀ (216 mg, 0.30 mmol), 4-anisaldehyde (20 mg, 0.15 mmol) and sarcosine (136 mg, 1.50 mmol) in toluene (60 mL) was warmed to reflux under an argon atmosphere and stirred for 26 h. The solvent was removed by distillation under reduced pressure. The crude product was purified by silica column chromatography (toluene/EtOAc, 99/1) to obtain fullerene **7** as a brown powder (78.8 mg, 60%). ¹H NMR (CDCl₃, 400 MHz): δ, ppm 7.69 (br s, 2 H), 6.95–6.93 (d, *J* = 8 Hz, 2 H), 4.97–4.95 (d, *J* = 8 Hz, 1 H), 4.87 (s, 1 H), 4.25–4.21 (d, *J* = 8 Hz, 1 H), 3.80 (s, 3 H, N-CH₃), 2.77 (s, 3 H, O-CH₃). MALDI-TOF MS (terthiophene): *m/z* calcd. for C₅₃H₄₈N₈O [M]⁺ 883.10, found 883.18.

Fulleropyrrolidine 8. To a solution of fullerene **7** (32 mg, 0.036 mmol) in toluene (20 mL) immersed in

ice-cold water, 1.5 mL of 1 M BBr_3 (1.5 mmol) was added dropwise. The mixture was stirred at room temperature for 24 h under an argon atmosphere. The mixture was then transferred to a separatory funnel and washed with water (30 mL \times 3) and then the solvent was removed by distillation under reduced pressure. The crude product was purified by column chromatography on silica gel (toluene/MeOH, 19/1) to obtain fullerene **8** as a brown solid (20 mg, 65%). $^1\text{H NMR}$ (CDCl_3 , 400 MHz): δ , ppm 7.65 (br s, 2 H), 6.85–6.83 (d, $J = 8$ Hz, 2 H), 4.97–4.95 (d, $J = 8$ Hz, 1 H), 4.86 (s, 1 H), 4.25–4.23 (d, $J = 8$ Hz, 1 H), 2.97 (s, 3 H). MALDI-TOF MS (terthiophene): m/z calcd. for $\text{C}_{69}\text{H}_{11}\text{NO}$ [$\text{M}]^+$ 869.08 found 869.15.

CONCLUSION

We report a new synthetic route to covalently linked phthalocyanine-fullerene dyads **1** and **1Zn**, and have shown that in toluene, $^1\text{ZnPc}-\text{C}_{60}$ rapidly equilibrates with $\text{ZnPc}-^1\text{C}_{60}$ by singlet–singlet energy transfer. These excited states decay mainly to the ground states of both chromophores and the phthalocyanine triplet state, as the fullerene triplet state transfers its triplet energy to the phthalocyanine. About 20% of the singlet excited states transfer an electron to the fullerene to generate $\text{ZnPc}^{+}\text{-C}_{60}^{-}$, which has a lifetime of 2.8 ns. In the more polar benzonitrile, the rate constant for photoinduced electron transfer increases dramatically, giving $\text{ZnPc}^{+}\text{-C}_{60}^{-}$ with a quantum yield of $\geq 85\%$. The lifetime of the charge separated state decreases in this solvent, in accord with Marcus theory. The 94 ps lifetime of $\text{ZnPc}^{+}\text{-C}_{60}^{-}$ in benzonitrile is almost 3 times longer than that for the corresponding state of a similar triad lacking the phenyl ring in the phthalocyanine-fullerene linkage. This is still short compared to lifetimes of charge separation in many porphyrin-fullerene and similar dyads, and longer lifetimes would be useful for the application of such dyads in solar energy conversion. Both charge separation and recombination are facilitated by the conjugation in the linkage joining the donor and the acceptor.

Acknowledgements

This work was supported by the Office of Basic Energy Sciences, Division of Chemical Sciences, Geosciences, and Energy Biosciences, Department of Energy under contract DE-FG02-03ER15393 and the Center for Bio-Inspired Solar Fuel Production, an Energy Frontier Research Center funded by the U.S. Department of Energy, Office of Science, Office of Basic Energy Sciences Under Award Number DE-SC0001016.

REFERENCES

- Gust D, Moore TA and Moore AL. *Faraday Discuss.* 2012; **155**: 9–26.
- Gust D and Moore TA. In *The Porphyrin Handbook*, Kadish KM, Smith KM and Guillard R. (Eds.) Academic Press: San Diego, 2000; pp 153–190.
- Meyer TJ. *Acc. Chem. Res.* 1989; **22**: 163–170.
- Redmore NP, Rubtsov IV and Therien MJ. *J. Am. Chem. Soc.* 2003; **125**: 8769–8778.
- Wasielewski MR. *Chem. Rev.* 1992; **92**: 435–461.
- Gust D, Moore TA and Moore AL. *Acc. Chem. Res.* 2001; **34**: 40–48.
- Falkenstrom M, Johansson O and Hammarstrom L. *Inorg. Chim. Acta* 2007; **360**: 741–750.
- Fukuzumi S and Imahori H. *Electron Transfer in Chemistry* 2001; **2**: 927–975.
- Flamigni L, Armaroli N, Barigelletti F, Balzani V, Collin J-P, Dalbavie J-O, Heitz V and Sauvage J-P. *J. Phys. Chem. B* 1997; **101**: 5936–5943.
- Gust D, Moore TA and Moore AL. *Acc. Chem. Res.* 2009; **42**: 1890–1898.
- Kobayashi N, Nakajima S and Osa T. *Inorg. Chim. Acta* 1993; **210**: 131–133.
- Tkachenko NV, Efimov A and Lemmetyinen H. *J. Porphyrins Phthalocyanines* 2011; **15**: 780–790.
- Isosomppi M, Tkachenko NV, Efimov A, Vahasalo H, Jukola J, Vainiotalo P and Lemmetyinen H. *Chem. Phys. Lett.* 2006; **430**: 36–40.
- Quintiliani M, Kahnt A, Woelfle T, Hieringer W, Vazquez P, Goerling A, Guldi DM and Torres T. *Chem. Eur. J.* 2008; **14**: 3765–3775.
- Kahnt A, Quintiliani M, Vazquez P, Guldi DM and Torres T. *ChemSuschem* 2008; **1**: 97–102.
- Quintiliani M, Kahnt A, Vazquez P, Guldi DM and Torres T. *J. Mater. Chem.* 2008; **18**: 1542–1546.
- Lemmetyinen H, Kumpulainen T, Niemi M, Efimov A, Ranta J, Stranius K and Tkachenko NV. *Photochem. Photobiol. Sci.* 2010; **9**: 949–959.
- Ince M, Victoria Martinez-Diaz M, Barbera J and Torres T. *J. Mater. Chem.* 2011; **21**: 1531–1536.
- Ranta J, Kaunisto K, Niskanen M, Efimov A, Hukka TI and Lemmetyinen H. *J. Phys. Chem. C* 2014; **118**: 2754–2765.
- El-Khouly ME, Kim JH, Kay KY and Fukuzumi S. *J. Porphyrins Phthalocyanines* 2013; **17**: 1055–1063.
- Urbani M, Osati S, Kuhri S, Guldi DM and Torres T. *J. Porphyrins Phthalocyanines* 2013; **17**: 501–510.
- Al-Subi AH, Efimov A, Niemi M, Tkachenko NV and Lemmetyinen H. *Chem. Phys. Lett.* 2013; **572**: 96–100.
- Kc CB, Ohkubo K, Karr PA, Fukuzumi S and D'Souza F. *Chem. Commun.* 2013; **49**: 7614–7616.
- Bottari G, Kahnt A, Guldi DM and Torres T. *ECS J. S. S. Sci. Tech.* 2013; **2**: M3145–M3150.
- Zhao H, Liu Z, Zhang X, Tian J, Chen C, Zhu Y and Zheng J. *Chin. J. Chem.* 2012; **30**: 1766–1770.
- Fukuda T, Kikukawa Y, Takaishi S and Kobayashi N. *Chem. Asian J.* 2012; **7**: 751–758.
- Enes RF, Cid JJ, Hausmann A, Trukhina O, Gouloumis A, Vazquez P, Cavaleiro JA, Tome AC,

- Guldi DM and Torres T. *Chem. Eur. J.* 2012; **18**: 1727–1736.
28. Ballesteros B, de la Torre G, Shearer A, Hausmann A, Angeles Herranz M, Guldi DM and Torres T. *Chem. Eur. J.* 2010; **16**: 114–125.
 29. Seitz W, Kahnt A, Guldi DM and Torres T. *J. Porphyrins Phthalocyanines* 2009; **13**: 1034–1039.
 30. Lemmetyinen H, Tkachenko N, Efimov A and Niemi M. *J. Porphyrins Phthalocyanines* 2009; **13**: 1090–1097.
 31. Fukuda T, Hashimoto N, Araki Y, El-Khouly ME, Ito O and Kobayashi N. *Chem. Asian J.* 2009; **4**: 1678–1686.
 32. Sukeguchi D, Yoshiyama H, Singh SP, Shibata N, Nakamura S, Toru T, Hayashi Y and Soga T. *Hetero. Commun.* 2009; **15**: 263–272.
 33. Kahnt A, Guldi DM, de la Escosura A, Martin-Diaz MV and Torres T. *J. Mater. Chem.* 2008; **18**: 77–82.
 34. Torres T, Gouloumis A, Sanchez-Garcia D, Jayawickramarajah J, Seitz W, Guldi DM and Sessler JL. *Chem. Commun.* 2007; 292–294.
 35. Chen Y, El-Khouly ME, Sasaki M, Araki Y and Ito O. *Org. Lett.* 2005; **7**: 1613–1616.
 36. Guldi DM, Zilbermann I, Gouloumis A, Vazquez P and Torres T. *J. Phys. Chem. B* 2004; **108**: 18485–18494.
 37. El-Khouly ME, Ito O, Smith PM and D'Souza F. *J. Photochem. Photobiol. C-Photochem. Rev.* 2004; **5**: 79–104.
 38. Loi MA, Denk P, Hoppe H, Neugebauer H, Meissner D, Winder C, Brabec CJ, Sariciftci NS, Gouloumis A, Vazquez P and Torres T. *Synth. Met.* 2003; **137**: 1491–1492.
 39. Gouloumis A, Liu SG, Sastre A, Vazquez P, Echegoyen L and Torres T. *Chem. Eur. J.* 2000; **6**: 3600–3607.
 40. Qiu WF, Liu YQ, Pan CY and Zhu DB. *Chinese Chemical Letters* 1997; **8**: 811–814.
 41. Liddell PA, Sumida JP, Macpherson AN, Noss L, Seely GR, Clark KN, Moore AL, Moore TA and Gust D. *Photochem. Photobiol.* 1994; **60**: 537–541.
 42. Bottari G, Olea D, Gomez-Navarro C, Zamora F, Gomez-Herrero J and Torres T. *Angew. Chem., Int. Ed.* 2008; **47**: 2026–2031.
 43. Förster T. *Disc. Faraday Soc.* 1959; **27**: 7–17.
 44. Williams RM, Zwier JM and Verhoeven JW. *J. Am. Chem. Soc.* 1995; **117**: 4093–4099.
 45. Lawrence DS and Whitten DG. *Photochem. Photobiol.* 1996; **64**: 923–935.
 46. Demas JN. *Excited State Lifetime Measurements*, Academic Press: New York, 1983; pp 59–61.
 47. Palacios RE, Kodis G, Gould SL, de la Garza L, Brune A, Gust D, Moore TA and Moore AL. *ChemPhysChem* 2005; **6**: 2359–2370.
 48. Marcus RA. *Can. J. Chem.* 1959; **37**: 155–163.
 49. Marcus RA. *J. Chem. Phys.* 1965; **43**: 679.
 50. Hush NS. *J. Electroanal. Chem.* 1999; **460**: 5–29.
 51. Hush NS. *Trans. Faraday Soc.* 1961; **57**: 557–580.
 52. Hush NS. *J. Chem. Phys.* 1958; **28**: 962–972.
 53. van Stokkum IHM, Larsen DS and van Grondelle R. *Biochem. Biophys. Acta* 2004; **1657**: 82–104.